JOURNAL OF OPTOELECTRONICS AND ADVANCED MATERIALS Vol. 10, No. 7, July 2008, p. 1819 - 1822

Magnetic and structural behaviour of $(Nd,Dy)_2Fe_{14}B/\alpha$-Fe nanocomposites obtained by mechanical milling and annealing

O. ISNARD[a], D. GIVORD[a], E. DOROLTI[b], V. POP[b*], L. NISTOR[b], A. TUNYAGI[b], I. CHICINAŞ[c]
[a]*Institut Néel, CNRS - Université Joseph Fourier, BP 166, 38042 Grenoble cedex 9, France*
[b]*Faculty of Physics, Babes-Bolyai University, 4000480 Cluj-Napoca, Romania*
[c]*Materials Sciences and Technology Dept., Technical University of Cluj-Napoca, 103-105 Muncii ave., 400641 Cluj-Napoca, Romania*

$(Nd_{0.92}Dy_{0.08})_2Fe_{14}B/\alpha$-Fe hard/soft magnetic nanocomposite have been obtained by mechanical milling in a high-energy planetary mill and subsequent annealing under vacuum. The influence of the milling and annealing conditions (temperature and time) on the structural and magnetic properties of $(Nd_{0.92}Dy_{0.08})_2Fe_{14}B/\alpha$-Fe nanocomposite have been investigated. Annealing at 550°C restores the magnetic features of the $Nd_2Fe_{14}B$ – type phase. The coercive field, remanent magnetization and the degree of the exchange coupling between the hard magnetic grains and the soft grains are strongly dependent on the milling time and the annealing conditions.

(Received April 1, 2008; accepted June 30, 2008)

Keywords: Nanocomposite magnetic materials, Exchange interactions, milling-annealing processes

1. Introduction

The study of the soft and hard nanocrystalline magnetic materials become one of the most dynamic research activity in material sciences, with direct applications in high density magnetic recording, permanent magnets, actuators, motors, sensors, etc. Nanocomposites exchange-enhanced hard magnetic materials have been intensively studied since their first experimental and theoretical description [1-7]. Skomski and Coey [8] first predicted that a giant energy product $(BH)_{max}$ over than 1 MJ/m^3 might be attainable in oriented exchange coupled $Sm_2Fe_{17}N_3/Fe_{65}Co_{35}$ nanocomposites. Similarly, a potential $(BH)_{max}$ of 720 kJ/m^3 was predicted in $Nd_2Fe_{14}B/\alpha$-Fe nanocomposite [9]. These values are about twice that of commercially available anisotropic permanent magnets (~ 400 kJ/m^3).

Kneller et *al*. [4] show that a mixture of nano-granular soft (Fe_3B or α-Fe), with a high magnetization, and hard ($Nd_2Fe_{14}B$) magnetic phases, with high coercivity coupled by exchange interaction can lead to an increase of the energy stored in the magnet up to $(BH)_{max}$ = 200 kJ/m^3. Beside the high energy gain of this materials one has to consider the thermal stability issues like the need of increase of the Curie temperature in order to assure a good stability of the magnet over a wide temperature range. Another important aspect is the one concerning the corrosion of the magnet in a moist and warm environment in this way preventing any microstructural change of the material. Considering the numerical simulations [10], the ideal average size of the nanocrystallites should be around 10 nm for the soft magnetic compound and about 20 nm for the hard magnetic phase. The difference between the theoretical computation and the values obtained is considered to be due to the limited possibilities of getting a good size distribution of the crystallites [11]. The crystallites sizes reported in the soft Fe_3B and α-Fe nano-granular material is larger than those used in the theoretical computation and the relatively low energetic value of the experimental BH_{max} [11-14] has been related to the non ideal microstructure. Of particular importance is that the average grain size of the soft magnetic phase in the nanocomposites has to be sufficiently small to ensure the exchange interactions between neighbouring grains [15]. As consequence of the short range feature of the exchange-coupling interaction between nanograins, the soft magnetic grains should be small enough, approximately twice the domain wall width of the hard magnetic phase [4, 16-17]. The grain sizes of the soft and hard magnetic phases constitute an important microstructural factor that critically influences the magnetic properties of the nanocomposite magnets.

Recently, by mechanical milling and annealing, we have successfully obtained hard/soft type magnetic nanocomposite with coercivity in a range of 3.7 – 8.2 kOe [18-20]. A few percent of Dy, substituted for Nd in the Nd-Fe-B hard magnetic phase proved to refine the microstructure and enhance the anisotropy field [21-23]. This increase of magnetic anisotropy favours on improvement of the coercivity. However, the presence of Dy decreases the saturation magnetization substantially as a consequence of the anti parallel coupling between Fe and Dy moments. High values for the maximum energy product could be obtained by remanence improving, keeping the coercivity sufficiently high. The exchange spring magnets, by exchange coupling of the hard and soft magnetic phases, represent an opportunity in this direction. In addition to our previous results concerning the

annealing influence on the structural and coercivity evolution of $(Nd_{0.92}Dy_{0.08})_2Fe_{14}B/\alpha$-Fe nanocomposite [18], in this paper we report our new results concerning thermal evolution of the magnetic phases and hysteresis behaviour vs. milling and annealing conditions.

2. Experimental

The mixture of 78 wt % $(Nd_{0.92}Dy_{0.08})_2Fe_{14}B$/22 wt % α-Fe was mechanically milled under argon atmosphere in a high-energy planetary mill. Several milling times were used ranging from 4 to 12 hours. The structure and the microstructure were tailored by appropriate heat treatments under vacuum between 450 and 800 °C from 5min to 14 hours. The experimental details are given elsewhere [18].

X-ray diffraction (XRD) was carried out on a Bruker D8 Advance diffractometer with Cu Kα radiation and a Siemens D500 powder diffractometer using the $K_{\alpha 1}$ radiation of copper (λ = 0.15406 nm) in the angular interval 2θ = 20 to 90°.

The phase analysis was done also from thermomagnetic measurements, measuring the Curie temperatures. The magnetic ordering temperatures were determined with a Faraday type balance in low magnetic field [18]. The magnetisation curves were recorded between 4 K and room temperature in a continuous magnetic field of up to 10 T by the extraction method [24].

3. Results and discussion

The XRD patterns of $(Nd_{0.92}Dy_{0.08})_2Fe_{14}B/\alpha$-Fe composite milled for 4 and 6 hours are presented in Figure 1a. The XRD patterns of the same samples annealed at 550 °C for 1.5 hours are presented in Figure 1b. The X-ray patterns for $(Nd_{0.92}Dy_{0.08})_2Fe_{14}B$ hard phase milled for 2 h and annealed at 550 °C for 1.5 hours are also given for comparison in Figure 1a and 1b respectively.

In our previously studies [18] of $(Nd_{0.92}Dy_{0.08})_2Fe_{14}B/\alpha$-Fe composite it was shown that the enlargement and almost disappearance of the diffraction peaks for high milling times can be attribute to the induced defects, the stresses induced by milling and to the decrease of the crystallites size. The annealing at appropriate temperatures, smaller than the recrystallization temperature, eliminates the defects and reduces the stresses. A comparison between three different samples milled for different periods and annealed at 550°C for 1.5 hours is shown in figure 1. The heat treatment at 550°C for 1.5 hours will refine the structure and no additional peaks were shown, Fig. 1b. These aspects prove that the initial phases present in composite were conserved after milling and annealing and no supplementary phases were fabricated. After annealing the width of the diffraction peaks decreases in comparison to the corresponding milled samples as a consequence of diminishing of the second order internal stresses and of the defects density. After 6 hours of milling the mean size of the *a*-Fe nanocrystallites, in the annealed samples, decrease to a mean value inferior to 30 nm, in accord with previous results [18, 25, 26]. On the contrary, annealing at 800°C for a short time (5 minutes) [18], shows rather narrow peaks which prove that this temperature is higher than the recrystallization temperature of the $Nd_2Fe_{14}B$ and α-Fe phases.

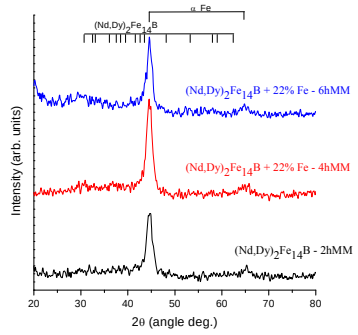

(a)

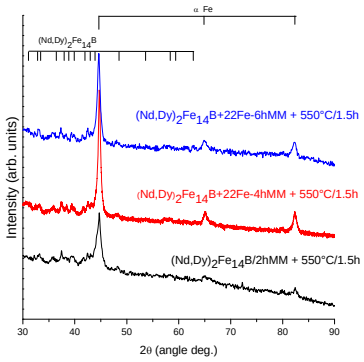

(b)

Fig. 1. X-ray diffraction patterns of the $(Nd_{0.92}Dy_{0.08})_2Fe_{14}B$ sample milled for 2 h and of the $(Nd_{0.92}Dy_{0.08})_2Fe_{14}B/\alpha$-Fe composite milled for 4 and 6 h; as milled samples (a) and annealed samples for the indicated time and temperature (b).

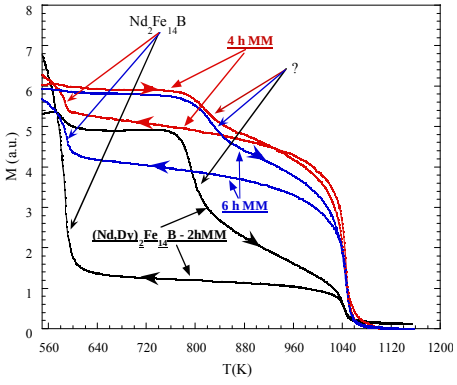

Fig. 2. Thermomagnetic curves of the $(Nd_{0.92}Dy_{0.08})_2Fe_{14}B$ hard phase milled for 2 hours and $(Nd_{0.92}Dy_{0.08})_2Fe_{14}B/\alpha$-Fe milled for 4 and 6 hours. The heating and cooling process are indicated by arrows.

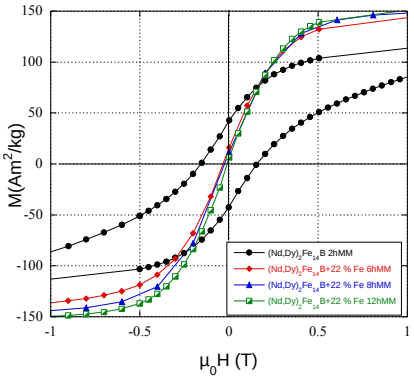

Fig. 3. Room temperature hysteresis cycles recorded for the $(Nd_{0.92}Dy_{0.08})_2Fe_{14}B/\alpha$-Fe composite samples milled for 6, 8 and 12 hours. The hysteresis cycles of $(Nd_{0.92}Dy_{0.08})_2Fe_{14}B$ hard phase milled for 2 hours is given for comparison.

The thermomagnetic curves, *M (T),* of $(Nd_{0.92}Dy_{0.08})_2Fe_{14}B$ hard phase milled for 2 hours and $(Nd_{0.92}Dy_{0.08})_2Fe_{14}B/\alpha$-Fe milled for 4 and 6 hours are given in figure 2. It can be seen that in the heating process from room temperature to 1200 K there is a magnetisation drop at about 595 K corresponding to the Curie temperature of the hard magnetic phase. Another step can be observed in the 800-900 K thermal range. This step could correspond to a milling induced phase which disappears after heat treatment. The third step corresponds to the Curie temperature of iron, 1043 K. As consequence of structural changes during the heating process, in the cooling process only two steps are detected. These two transitions correspond to the starting phases in the mixture before milling: $(Nd_{0.92}Dy_{0.08})_2Fe_{14}B$ and α-Fe. This result confirms that no supplementary phases were fabricated by milling and annealing, result in good agreement with X-ray studies shown in figure 1.

The hysteresis curves at 300 K for $(Nd_{0.92}Dy_{0.08})_2Fe_{14}B$ hard phase milled for 2 h and $(Nd_{0.92}Dy_{0.08})_2Fe_{14}B/\alpha$-Fe composite milled for 6, 8 and 12 hours are plotted in figure 3. It is clearly evidenced the missing of the coercivity in as milled composite samples. The missing of the coercivity can be explained by the strong diminish of the anisotropy of the hard magnetic phases as result of the poor crystalline order detected after milling, figure 1. The annealing of the milled samples succeeds to restore the crystalline structure, figure 1b. This fact results in a strong increasing of the remanence and coercivity in the annealed samples, figure 4. Higher milling times induce a slow decrease of the magnetic properties of the composite samples annealed at 550°C for 1.5 h. This evolution can be correlated with the structural evolution. Consequently, an appropriate correlation between milling time and annealing conditions is necessary in order to obtain optimum magnetic properties as result of an optimisation of the structure and microstructure and diminishing the defect density. The hysteresis curves of the $(Nd_{0.92}Dy_{0.08})_2Fe_{14}B/\alpha$-Fe nanocomposites 6 h milled and annealed at 800 °C show a clear decoupling between the soft and hard magnetic phases [18]. This behaviour is explained by the strong increasing of the crystallites size after annealing at 800°C as it was evidenced from X-ray diffraction.

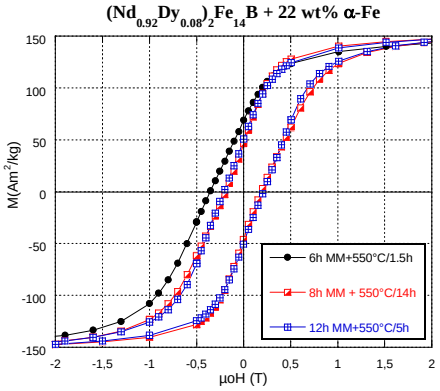

Fig. 4. Room temperature hysteresis cycles recorded for the $(Nd_{0.92}Dy_{0.08})_2Fe_{14}B/\alpha$-Fe composite samples milled for 6, 8 and 12 h annealed at 550°C for 1.5 h.

Table 1. M (under a field of 10 T), M_R and H_C values, at 300 K, of the $(Nd_{0.92}Dy_{0.08})_2Fe_{14}B$ hard phase milled for 2 hours and of $(Nd_{0.92}Dy_{0.08})_2Fe_{14}B/\alpha$-Fe composites milled for 6, 8 and 12 h before and after a heat treatment at 550°C/1.5 h.

Sample	Milling time (h)	Annealing Temperature (°C)	M (Am^2/kg)	M_R (Am^2/kg)	H_C (kOe)
$(Nd_{0.92}Dy_{0.08})_2Fe_{14}B$	2	-	140	43	1.5
$(Nd_{0.92}Dy_{0.08})_2Fe_{14}B$	2	550	145	54	2.5
$(Nd_{0.92}Dy_{0.08})_2Fe_{14}B/$ α-Fe	6	-	157	17	0.35
$(Nd_{0.92}Dy_{0.08})_2Fe_{14}B/$ α-Fe	6	550	163	70	3.7
$(Nd_{0.92}Dy_{0.08})_2Fe_{14}B/$ α-Fe	8	-	160	12	0.27
$(Nd_{0.92}Dy_{0.08})_2Fe_{14}B/$ α-Fe	8	550	161	46	1.9
$(Nd_{0.92}Dy_{0.08})_2Fe_{14}B/$ α-Fe	12	-	161	7	0.1
$(Nd_{0.92}Dy_{0.08})_2Fe_{14}B/$ α-Fe	12	550	162	49	2.1

A summary of the obtained magnetisation values at 10 T, M, the coercive field, Hc, and the remanence, M_R, is given in table 1. The $(Nd_{0.92}Dy_{0.08})_2Fe_{14}B$ hard phase milled for 2 hours has a magnetisation of about 140 Am^2/kg under a field of 10 T. By co-milling the hard $(Nd_{0.92}Dy_{0.08})_2Fe_{14}B$ phase with the Fe soft magnetic phases, an enhancement of the saturation magnetisation is observed (Table 1). After a heat treatment at 550 °C of the as milled $(Nd_{0.92}Dy_{0.08})_2Fe_{14}B/\alpha$-Fe composite samples for different milling times, the saturation magnetisation at 10 T increases up to 163 Am^2/kg for 6 h of milling (Table 1).

4. Conclusions

Mechanical milling and annealing has been applied in order to obtain 78 wt % $(Nd_{0.92}Dy_{0.08})_2Fe_{14}B$/22 wt % α-Fe exchange coupled magnetic nanocomposite. The influence of the milling and the annealing conditions on the structural and magnetic behaviour of the $(Nd_{0.92}Dy_{0.08})_2Fe_{14}B/\alpha$-Fe composite powder has been studied. The annealing conditions have a direct influence on the efficiency of the exchange coupling between hard and soft magnetic phases.

Heat treatments at 550 °C on the powder milled for 6, 8 and 12 hours refine the crystal structure and increase both the remanence and the coercivity. Based on the XRD result and magnetic measurements, it is believed that in $(Nd_{0.92}Dy_{0.08})_2Fe_{14}B/\alpha$-Fe composite sample milled for 6 hours and annealed at 550°C for 1.5 h the exchange coupling between the hard and soft magnetic phases is optimal. The coercivity and the remanence decrease for the nanocomposite samples milled for 8 and 12 h, which prove that the milling times are too long or the annealing conditions are not appropriate for obtaining an optimum exchange coupling between nanocrystallites. Further investigations are in progress in order to well understand these evolutions and to increase magnetic properties toward the theoretical predictions.

Acknowledgment

This work has been partly supported by the CEEX and CNCSIS grants.

References

[1] R. Coehoorn, D. B. de Mooij, J. P. W. B. Duchateau, K. H. J. Buschow, J. de Phys. **49,** C8-669 (1988).
[2] R. Coehoorn, D. B. Mooij and D. de Woord, J.Magn. Magn. Mater. **80**, 101 (1989)
[3] D. Eckert, A. Handstein, K-H. Muller, R. Hecske, J. Schneider, N. Mattern, L. Illgen, Matter. Let. **9**, 289-293 (1990).
[4] E. Kneller, R. Hawig, IEEE Trans. Magn. **27,** 3588 (1991).
[5] A. Manaf, R. A. Buckley, and H. A. Davies, J. Magn. Magn. Mater. **128**, 302 (1993)
[6] V. Neu and L. Schultz, J. Appl. Phys. **90,** 1540 (2001)
[7] I. Betancourt, H. A. Davies, Appl. Phys. Lett. **87,** 162516 (2005)
[8] R. Skomski, J. M. D. Coey, Phys. Rev. B **48,** 15812 (1993)
[9] T. Lieneweber, H. Kronmuller J. Magn. Magn. Mater. **176**, 145 (1997)
[10] I. Betancourt, and H. A. Davies, Appl. Phys. Letters, **87**, 162516 (2005).
[11] G. C. Hadjipanayis, J. Magn. Magn. Mater. **200**, 373 (1999).
[12] H. W. Zhang, S. Y. Zhang, and B. G. Shen, J. Appl. Phys. **85**, 4660 (1999).
[13] P. G. McCormick, W. F. Miao, P. A. I. Smith, J. Ding, R. Street, J. Appl. Phys. **83**, 6256 (1998).
[14] L. Withanawasam, A. S. Murthy, and G. C. Hadjipanayis, IEEE Trans. Magn. **31**, 3608 (1995).
[15] R. Fischer, T. Schrefl, H. Kronmuller, and J. Fidler, J. Magn. Magn. Mater. **153**, 35 (1996)
[16] T. Schrefl, H. Kronmuller, and J. Fidler, Phys. Rev. B **49,** 6100 (1994)
[17] B. Z. Cui, X. K. Sun, W. Liu, Z. D. Zhang, D. Y. Geng, X. G. Zhao, J. Phys. D **33**, 338-344 (2000)
[18] E. Dorolti, V. Pop, O. Isnard, D. Givord, I. Chicinaş, J. Optoelectron. Adv. Mater. **9**, 1474 (2007).
[19] V. Pop, O. Isnard, I. Chicinaş, D. Givord, J. M. Le Breton, Journal of Optoelectronics and Advanced Materials **8** (2006) 494.
[20] V. Pop, O. Isnard, I. Chicinaş, D. Givord J. Magn. Magn. Mat. **310** (2007) 2489-2490
[21] M. Sagawa, S. Hirosawa, K. Tokuhara, H. Yamamoto, S. Fujimura, Y. Tsubokawa, R. Shimizu, J. Appl. Phys. **61,** 3559 (1987)
[22] Z. Liu, H. A. Davies, J. Magn. Magn. Mater. **290-291,** 1230-1233 (2005)
[23] B. E. Meacham, D. J. Branagan, J. E. Shield J. Magn. Magn. Mater. **277,** 123-129 (2004)
[24] A. Barlet, J. C. Genna, P. Lethuillier, Cryogenics **31,** 801 (1991)
[25] C. Y. You, X. K. Sun, L. Y. Xiong, W. Liu, B. Z. Cui, X. G. Zhao, D. Y. Geng, Z. D. Zhang, J. Magn. Magn. Mater. **268**, 403 (2004).
[26] W. F. Miao, J. Ding, P. G. McCormick, R. Street, J. Phys. D: Appl. Phys. **29,** 2371 (1996)

*Corresponding author: viorel@phys.ubbcluj.ro